Elliptic incoherent solitons in saturable nonlinear media

Eugenia D. Eugenieva* and Demetrios N. Christodoulides

Department of Electrical Engineering and Computer Science, Lehigh University, Bethlehem, Pennsylvania 18015

Mordechai Segev

Department of Physics, Technion Institute of Technology, Haifa 32000, Israel, and Department of Electrical Engineering, Princeton University, Princeton, New Jersey 08544

Received March 6, 2000

We identify elliptic incoherent spatial solitons in isotropic saturable nonlinear media. These solitary states are possible, provided that their correlation function is anisotropic. The propagation dynamics of this new class of solitons are investigated by use of numerical simulations. We find that, during a collision event of two such elliptic solitons, their intensity ellipse rotates, and at the same time their centers of gravity tend to revolve around each other. © 2000 Optical Society of America

OCIS codes: 190.5330, 190.5530, 190.4420.

Since their first experimental observation, spatial incoherent solitons have been the focus of considerable attention.[1] In general, spatial incoherent solitons are multimode self-trapped entities, which are possible only in materials with noninstantaneous nonlinearities. Thus far, the theory of incoherent spatial solitons has proceeded along three paths: (i) the coherent density method,[2–4] (ii) self-consistent multimode theory,[5–7] and (iii) the mutual coherence function propagation method.[8] Approximate ray-transport methods also exist that are valid in the case of very broad incoherent beams.[9–11] Analytically, incoherent Gaussian spatial solitons were first demonstrated in systems with logarithmic nonlinearities,[3] in which the strong link between the properties of these self-trapped soliton solutions and their correlation statistics became apparent. The self-focusing collapse of two-dimensional incoherent beams in Kerr nonlinear media was also recently investigated,[12] along with the modulation instability properties of incoherent wave packets.[13]

It is well known that two-dimensional coherent solitons are always circular in materials with isotropic saturable nonlinearities. Furthermore, if a coherent elliptic beam is launched into an isotropic self-focusing medium, the beam always undergoes significant oscillations in the transverse plane.[14] In other words, isotropic nonlinear media cannot support coherent elliptic solitons. Very recently, however, elliptic incoherent solitons were theoretically predicted in saturable nonlinear media of the logarithmic type.[6] These solitons were found to be possible, provided that their correlation function is appropriately anisotropic. It is therefore natural to ask whether such elliptic incoherent entities exist in general in other nonlinear systems besides the logarithmic. These other systems may include, for example, biased photorefractive crystals and materials with thermal nonlinearities. Even more importantly, at this point, there is to our knowledge no information whatsoever regarding the propagation dynamics and collision properties of such incoherent elliptic soliton entities.

In this Letter we identify elliptic incoherent solitons in isotropic saturable nonlinear media. We do this by employing a two-dimensional version of the coherent density approach[2–4] and by assuming that the material nonlinearity depends on the optical intensity I in a way similar to that in photorefractives (i.e., $\Delta n_{\rm nl} \propto 1/1+I$). We find that, even in this case, elliptic solitary states exist, provided that their mutual coherence function is anisotropic. Therefore these soliton states can possibly be excited from anisotropic incoherent sources such as edge-emitting LED's or lasers operated below threshold.[15] The propagation dynamics of this new class of solitons are further studied by use of numerical simulations. Collisions between two such elliptic incoherent solitons are also investigated. In particular, we show that in certain collision regimes the intensity ellipse for the two solitons rotates, whereas at the same time their centers of gravity tend to revolve around each other. This interaction behavior is possible even though these states are launched parallel to the propagation axis.

Following Refs. 2–4, we note that the coherent density function $f(x,y,z,\theta_x,\theta_y)$ evolves according to

$$i\left[\frac{\partial f}{\partial z}+\left(\theta_x\frac{\partial f}{\partial x}+\theta_y\frac{\partial f}{\partial y}\right)\right]+\frac{1}{2k}\nabla_\perp{}^2 f - \frac{k\Delta n}{n_0(1+I_N)}f=0\,, \quad (1)$$

$$I_N=\int_{-\infty}^{\infty}\int_{-\infty}^{\infty}|f(x,y,z,\theta_x,\theta_y)|^2 \mathrm{d}\theta_x \mathrm{d}\theta_y\,, \quad (2)$$

where, at the origin $z=0$,

$$f(x,y,0,\theta_x,\theta_y)=r^{1/2}G_N{}^{1/2}(\theta_x,\theta_y)\Phi_0(x,y)\,. \quad (3)$$

In Eqs. (1)–(3), $k=2\pi n_0/\lambda_0$ is the wave number, n_0 is the linear refractive index, Δn is the maximum nonlinear refractive-index change, and $I_N=I/I_S$ is the normalized intensity with respect to the saturation intensity. The intensity ratio r is defined as $r=I_{\max}/I_S$, and $I_{\max}$ is the initial maximum beam intensity. θ_x and θ_y represent the angles at which the density propagates with respect to the propagation direction in the (xz) and

(yz) planes, respectively, and $G_N(\theta_x, \theta_y)$ is the normalized angular power spectrum of the incoherent beam [i.e., $\int_{-\infty}^{\infty}\int_{-\infty}^{\infty} G_N(\theta_x, \theta_y)\mathrm{d}\theta_x \mathrm{d}\theta_y = 1$]. $\Phi_0(x, y)$ is a spatial modulation function, and for simplicity we assume here a Gaussian distribution for $G_N(\theta_x, \theta_y)$, i.e.,

$$G_N(\theta_x, \theta_y) = (\pi \theta_{0x} \theta_{0y})^{-1} \exp\left(-\frac{{\theta_x}^2}{{\theta_{0x}}^2} - \frac{{\theta_y}^2}{{\theta_{0y}}^2}\right), \quad (4)$$

where θ_{0x} and θ_{0y} are associated with the widths of the angular power spectrum in the x and y directions, respectively. Equations (1)–(4) were solved with a multiple-beam-propagation method program.[2] In all cases presented in this Letter, 625 components (on a rectangular grid) were used. The accuracy of the method was checked against the elliptic analytical solutions reported in Ref. 6.

In the examples to follow, we consider elliptic partially incoherent Gaussian beams, whose initial spatial modulation function is given by $\Phi_0(x, y) = \exp\{-(1/2)[(x/\omega_{0x})^2 + (y/\omega_{0y})^2]\}$, where ω_{0x} and ω_{0y} are associated with the beam widths along the x and y axes.

As a first example, let us study the evolution of a circular partially coherent Gaussian beam. The spot size of this beam is $\omega_0 = 10$ μm (its intensity FWHM is 16 μm), $r = 3$, and $\theta_{0x} = \theta_{0y} = 0.4°$. The free-space wavelength is taken here to be $\lambda_0 = 0.448$ μm, and the refractive index is $n_0 = 2.3$. In the absence of any nonlinearity, this beam expands to a FWHM of 388 μm after a distance of 3 cm. Conversely, in the nonlinear regime, computer simulations indicate that stable self-trapping is achieved when the maximum nonlinear index change is approximately $\Delta n \cong 3.15 \times 10^{-4}$. For this set of values the intensity fluctuations remain very small during propagation, which in turn indicates that a quasi soliton has been formed. We have also found that a departure from this set of values (nonlinearity, ω_0, θ_0) leads to breathing behavior, during which the beam continually expands and contracts. This observation is in agreement with recently found behavior in logarithmic nonlinear media.[16]

Next, we consider an elliptic partially coherent beam with beam widths $\omega_{0x} = 20$ μm (33 μm FWHM) and $\omega_{0y} = 9$ μm (15 μm FWHM). Our simulations indicate that, when the angular widths are $\theta_{0x} = 0.283°$ (4.93 mrad) and $\theta_{0y} = 0.2°$ (3.5 mrad), stable self-trapping of this elliptic beam can be achieved, provided that the nonlinear index change is $\Delta n \approx 1.42 \times 10^{-4}$. Figures 1a and 1b show the intensity evolution of this elliptic incoherent beam along the x and y cross sections, respectively, to a distance of 4 cm. Figures 1c and 1d depict the input and output intensity distributions of this soliton beam. Again, during propagation the intensity profile remains almost unchanged, indicating that a quasi soliton has been formed. Note that this stationary elliptic soliton is possible in spite of the isotropic nature of the nonlinearity that is assumed. Instead this soliton owes its existence to the anisotropic coherence function. When the nonlinear index change is different from the one used in the latter example (say, $\Delta n \cong 2.84 \times 10^{-4}$) or when the incoherent source is isotropic (e.g., $\theta_{0x} = \theta_{0y} = 0.2°$), the initially elliptic beam undergoes substantial oscillations in terms of its intensity and width. To understand better the formation of such elliptic incoherent solitons, we may find it useful to discuss first their diffraction properties. In the linear regime the spot size of a Gaussian–Schell beam along x and y (ω_x and ω_y) expands according to[6] $\omega_{x,y}(z) = \omega_{0x,y}[1 + (1 + {V_{x,y}}^2)(z/k{\omega_{0x,y}}^2)^2]^{1/2}$, where $V_{x,y} = k\omega_{0x,y}\theta_{0x,y}$. For the particular example considered above ($\theta_{0x} = 0.283°$, $\theta_{0y} = 0.2°$, $\omega_{0x} = 20$ μm, $\omega_{0y} = 9$ μm, $n_0 = 2.3$, $\lambda_0 = 0.488$ μm), the $x-y$ beam widths of this elliptic beam become $\omega_x \approx \omega_y \approx 105$ μm after 2 cm. Thus, in the linear regime, after 2 cm this elliptic formation diffracts to a beam of almost circular shape, as shown in Fig. 2e. In essence, this diffraction is equivalent to self-trapping of coherent circular solitons (the diffraction of which is isotropic), where isotropic diffraction results from proper engineering of the coherence properties of this elliptic beam. Similar conclusions could have been derived analytically from the logarithmic model.[6] Note that if this same beam were totally coherent, because of diffraction the beam widths would have expanded to $\omega_x = 39$ μm and $\omega_y = 76$ μm after the same propagation distance (2 cm); i.e., in the far field, the intensity ellipse will flip by 90°.

Next we investigate interactions between two such elliptic incoherent solitons. We first assume that the centers of two such solitons (those shown in Fig. 1) are located on the y axis and are 28 μm apart. These solitons are mutually incoherent with respect to each other; their major axes are parallel to the x direction and are launched parallel to the z axis. In this case our simulations show that these solitons continuously coalesce and separate during propagation in a way similar to what one may have expected from the interaction of two circular solitons. An interesting collision regime arises when the two beams are allowed to interact when their major axes are initially tilted

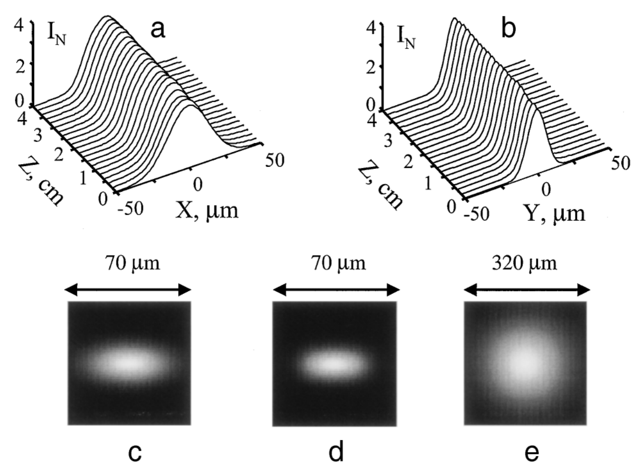

Fig. 1. Intensity evolution of an elliptic Gaussian soliton beam when $r = 3$, $\theta_{0x} = 0.283°$, $\theta_{0y} = 0.2°$, and $\Delta n = 1.42 \times 10^{-4}$: a, along the x axis; b, along the y axis. Gray-scale images: c, input and d, output elliptic soliton and e, its diffraction after 2 cm.

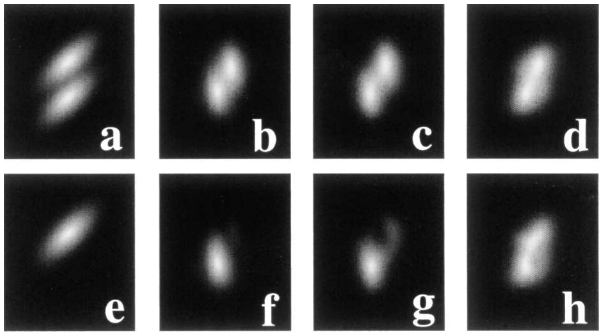

Fig. 2. Gray-scale images of (a–d) the total intensity distribution and (e–h) the intensity distribution of a single elliptic soliton beam at (a, e) $z = 0$ cm, (b, f) $z = 1.6$ cm, (c, g) $z = 2.12$ cm, and (d, h) $z = 4.7$ cm.

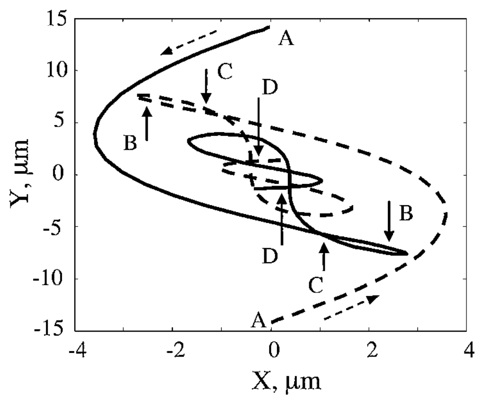

Fig. 3. Trajectories of the centers of gravity in the transverse plane of two elliptic soliton beams initially centered on the y axis and tilted at 45° with respect to x axis. Points A, B, C, and D occur at z values of 0, 1.6, 2.12, and 4.7 cm, respectively.

(Fig. 2a). The elliptic solitons considered are again those shown in Fig. 1. The distance between their centers is 28 μm, and their major axes are tilted by 45° with respect to x. Figure 2 shows gray-scale images of (a–d) the total intensity and (e–h) the intensity of a single soliton beam up to a distance of ≈ 5 cm. The size of the windows depicted is 100 μm $\times$ 125 μm. In this case, the off-axis interaction generates a torque on each elliptic incoherent soliton, which in turn tends to rotate them around their center. This is clear in Figs. 2f (at $z = 1.6$ cm) and 2g (at $z \approx 2.12$ cm), where the two ellipses have rotated by more than 45°. We point out that this rotation is unique to the elliptic character of these incoherent soliton beams, since it is totally absent in interactions involving circular solitons. The position of the gravity center of each beam is shown in Fig. 3. The dashed arrows show the direction along the trajectory. As before, initially the two solitons continuously coalesce and separate during propagation, and they almost fuse near 5 cm. The beginning of this fusion process can be seen in Fig. 2g, in which some light from one elliptic soliton starts to leak toward the other. This effect becomes more pronounced later at $z \approx 4.7$ cm. It is also clear from Fig. 3 that the centers of the solitons tend to rotate around the overall center of gravity of the total intensity distribution [(0, 0) point]. Unlike with spiraling involving coherent solitons,[17] this rotation occurs even though the two beams are launched parallel to the z axis.

In conclusion, we have identified elliptic partially incoherent solitons in saturable nonlinear media. These soliton states are possible by proper engineering of their coherence function. We found that during a collision event of two such elliptic solitons their intensity ellipse rotates and at the same time their centers of gravity tend to revolve around each other.

E. Eugenieva acknowledges support from National Science Foundation (NSF)–NATO Fellowship in Science and Engineering. This research was supported in part by the U.S. Air Force Office of Scientific Research, the NSF, and the U.S. Army Research Office and by a grant from the Pittsburgh Supercomputing Center.

*Permanent address, Institute of Electronics, Bulgarian Academy of Sciences, 72 Tzarigradsko Shosse, Sofia 1784, Bulgaria.

References

1. M. Mitchell, Z. Chen, M. Shih, and M. Segev, Phys. Rev. Lett. **77,** 490 (1996).
2. D. N. Christodoulides, T. H. Coskun, M. Mitchell, and M. Segev, Phys. Rev. Lett. **78,** 646 (1997).
3. D. N. Christodoulides, T. H. Coskun, and R. I. Joseph, Opt. Lett. **22,** 1080 (1998).
4. T. H. Coskun, D. N. Christodoulides, M. Mitchell, Z. Chen, and M. Segev, Opt. Lett. **23,** 418 (1998).
5. M. Mitchell, M. Segev, T. H. Coskun, and D. N. Christodoulides, Phys. Rev. Lett. **79,** 4990 (1997).
6. D. N. Christodoulides, T. H. Coskun, M. Mitchell, and M. Segev, Phys. Rev. Lett. **80,** 2310 (1998).
7. N. Akhmediev, W. Krolikowski, and A. W. Snyder, Phys. Rev. Lett. **81,** 4632 (1998); W. Krolikowski, N. Akhmediev, and B. Luther-Davies, Phys. Rev. E **59,** 4654 (1999).
8. G. A. Pasmanik, Sov. Phys. JETP **39,** 234 (1974); V. A. Aleshkevich, S. S. Lebedev, and A. N. Matveev, Sov. J. Quantum Electron. **11,** 647 (1981).
9. A. Hasegawa, Phys. Fluids **18,** 77 (1975).
10. A. W. Snyder and D. J. Mitchell, Phys. Rev. Lett. **80,** 1422 (1998).
11. V. V. Shkunov and D. Z. Anderson, Phys. Rev. Lett. **81,** 2683 (1998).
12. O. Bang, D. Edmundson, and W. Krolikowski, Phys. Rev. Lett. **83,** 5479 (1999).
13. M. Soljacic, M. Segev, T. H. Coskun, D. N. Christodoulides, and A. Vishwanath, Phys. Rev. Lett. **84,** 467 (2000).
14. B. Crosignani and P. Di Porto, Opt. Lett. **18,** 1394 (1993); A. W. Snyder and D. J. Mitchell, Opt. Lett. **22,** 16 (1997); V. Tichonenko, Opt. Lett. **23,** 594 (1998).
15. H. Kressel, M. Ettenberg, J. P. Wittke, and I. Ladany, in *Semiconductor Devices for Optical Communication,* H. Kressel, ed. (Springer-Verlag, New York, 1980), Chap. 2.
16. W. Krolikowski, D. Edmundson, and O. Bang, Phys. Rev. E **61,** 3122 (2000).
17. M. Shih, M. Segev, and G. Salamo, Phys. Rev. Lett. **78,** 2551 (1997); A. Buryak, Yu. S. Kivshar, M. Shih, and M. Segev, Phys. Rev. Lett. **82,** 81 (1999); A. Stepken, M. R. Belic, F. Keiser, W. Krolikowski, and B. Luther-Davies, Phys. Rev. Lett. **82,** 540 (1999).